Parameter Design of High Speed Coupling for 6 MW Wind Turbine Considering Torsional Vibration

JongHun Kang[1], Junwoo Bae[2], Seungkeun Jeong[3] , SooKeun Park[4] and Hyoung Woo Lee[1] #

Abstract

This article discusses parameter design of a high-speed coupling for 6 MW wind power generators considering torsional vibration. Modeling of a high-speed coupling for 6 MW wind power generators was performed using the transfer matrix method; parameter design was performed with regard to the torsional stiffness of a glass fiber reinforced plastic (GRFP) spacer and a high-speed coupling disc pack to cause the first natural frequency to be over 2,000 rpm. When the optimal torsional stiffness of the GFRP spacer was 2,400 to 2,500 KN·m/rad, and that of the disk pack was 32,000 to 39,000 KN·m/rad, the first natural frequency was over 2,000 rpm. Structural analysis was performed at disk pack thicknesses of 6 T to 10 T; the optimal torsional stiffness was found at 10 T. Structural analysis was performed with two to four sheets of the disk pack, having a thickness of 3 T: the optimal result was found with three disk pack sheets having a thickness of 3 T. ANSYS modeling and critical speed analysis, performed using the design parameters for the GFRP spacer and the disc pack, showed that no critical speed existed and the first natural frequency was over 2,000 rpm at a maximum operating speed of 1,500 rpm, verifying the validity of the parameters.

Keywords: 6 MW Wind Turbine, Torsional Vibration, High Speed Couplig, Parameter Design, Critical Speed, Torsional Stiffness

INTRODUCTION

A high-speed coupling for wind power generators, shown in Figure 1, is placed between a gearbox and a generator to transmit the power and absorb the distance variation and axial misalignment between the gearbox and the generator. In addition, a high-speed coupling for wind power generators has an insulating function, preventing electric corrosion caused by flow of current from the generator to the gearbox; it also prevents the transmission to the gearbox from overloading, which may be caused by abrupt power failure. A high-speed coupling for wind power generators is one of the core parts of wind power generators, of which the design, functions, and part verification are described in the IEC61400 and GL Guidelines, wherein it can be found that the part must have a durability life of 20 years or longer under distance variation and axial misalignment between the gearbox and the generator [1-3]. Therefore, under the conditions of maximum displacement and maximum allowable torque shown in Figure 2, the design and the service coefficient should meet the DIN740-2 standards for flexible coupling [4]. In addition, for commercial power generation using wind power generators, torsional stiffness design for each part is necessary to prevent resonance due to the torsional vibration of the power transmission system in the rotation range.
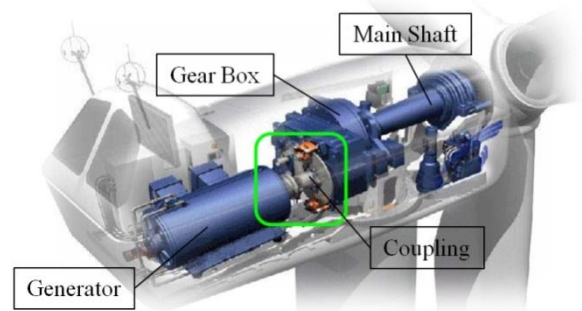

Figure 1: Tapered joint of wind turbine coupling (3)

The stress and safety factors of industrial couplings, including couplings for wind power generators, at maximum displacement are topics of general structural mechanics that are applied to representative couplings such as gear couplings and disk couplings [5-7].

In the present study, for the parameter design of a high-speed coupling for 6 MW wind power generators, modeling of a high-speed coupling was performed using the transfer matrix method; the parameters of the high-speed coupling were designed to cause the first natural frequency to be over 2,000 rpm. In addition, optimal GFRP spacer and disc pack parameters for the designed high-speed coupling were derived. The design parameters of the GFRP spacer and the disc pack were used to perform ANSYS modeling and an analysis of the critical speed for mass imbalance, through which the validity

of the parameter design for the high-speed coupling was verified [8-11].

HIGH SPEED COUPLING ROTOR DYNAMICS MODEL

Methods of analyzing the vibration of rotating machines are classified into the transfer matrix method and the finite element method. The transfer matrix method requires a degree of freedom much smaller than that of the finite element method and may be easily applied to a general shape.

The transfer matrix method includes three procedures. First, a system is divided into elements, and a local transfer matrix is calculated for each element. Second, a transfer matrix relation is obtained between the first and final state vectors. The transfer matrix relation between the first and final state vectors is obtained as a product of consecutive local transfer matrices. Finally, the boundary conditions for both ends of the system are applied. As a result, algebraic equations are expressed with the initial state variables.

Figure 2 shows the transfer matrix model for the torsional vibration analysis of a high-speed coupling. In Figure 2, the starting point and the end point of each element are referred to as stations, and each element is referred to as a field. The torsional stiffness of a high speed coupling was analyzed using the transfer matrix method.
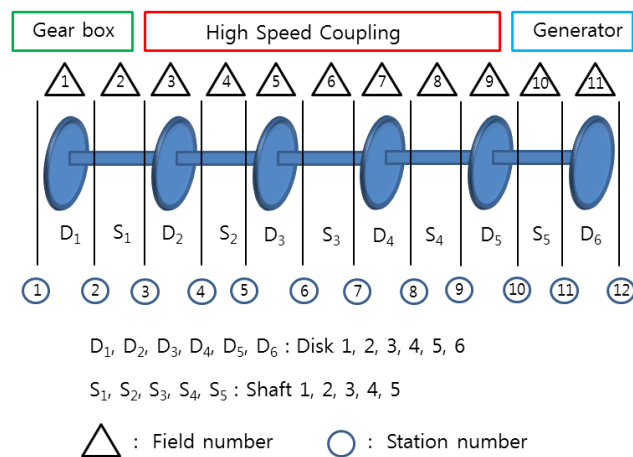

$D_1, D_2, D_3, D_4, D_5, D_6$: Disk 1, 2, 3, 4, 5, 6

S_1, S_2, S_3, S_4, S_5 : Shaft 1, 2, 3, 4, 5

△ : Field number   ◯ : Station number

Figure 2: Torsional vibration model of a high speed coupling.

High Speed Coupling Stiffness Parameter Design

Table 1 shows the specifications for the high-speed coupling stiffness parameter design considering torsional vibration: the disc pack torsional stiffness values, Kt_2 and Kt_4, were varied from 5,000 to 39,000 KN·m/rad and the GFRP spacer torsional stiffness value, Kt_3, was varied from 600 to 4,400 KN·m /rad. Because it was difficult to increase the stiffness of the GRFP spacer, optimal torsional stiffness design was performed by keeping the disc pack stiffness high and the

GRFP spacer stiffness low. As the maximum rotational speed of the 6 MW high-speed coupling was 1,500 rpm, the goal of the design was to cause the first natural frequency to be over 2,000 rpm. Figure 3 shows the critical speed map obtained by varying Kt3 from 600 to 4,400 KN·m/rad at the Kt_2 and Kt_4 values of 5,000 KN·m/rad, 7,000KN·m/rad, 9,000 KN·m/rad, and 11,000 KN·m/rad. When Kt_2 and Kt_4 were 11,000 KN·m/rad and Kt_3 was over 3,397 KN·m/rad, the first natural frequency was over 2,000 rpm. Figure 4 shows the critical speed map obtained by varying Kt_3 from 600 to 4,400 KN·m/rad at the Kt_2 and Kt_4 values of 13,000 KN·m/rad, 15,000 KN·m/rad, 17,000 KN·m/rad, and 19,000 KN·m/rad. When Kt_2 and Kt_4 were 19,000 KN·m/rad and Kt_3 was over 2,716 KN·m/rad, the first natural frequency was over 2,000 rpm. Figure 5 shows the critical speed map obtained by varying Kt_3 from 600 to 4,400 KN·m/rad at the Kt_2 and Kt_4 values of 21,000 KN·m/rad, 23,000 KN·m/rad, 25,000 KN·m/rad, and 27,000 KN·m/rad. When Kt_2 and Kt_4 were 27,000 KN·m/rad and Kt_3 was over 2,512 KN·m/rad, the first natural frequency was over 2,000 rpm. Figure 6 shows the critical speed map obtained by varying Kt_3 from 600 to 4,400 KN·m/rad at the Kt_2 and Kt_4 values of 29,000 KN·m/rad, 31,000 KN·m/rad, 33,000 KN·m/rad, 35,000 KN·m/rad, 37,000 KN·m/rad, and 39,000 KN·m/rad. When Kt_2 and Kt_4 were 29,000 KN·m/rad and Kt_3 was over 2,380 KN·m/rad, the first natural frequency was over 2,000 rpm. In addition, when Kt_2 and Kt_4 were 29,000 KN·m/rad and Kt_3 was over 2,490 KN·m/rad, the first natural frequency was over 2,000 rpm. Therefore, the optimal Kt_3 was found to be from 2,400 to 2,500 KN·m/rad and that of Kt_2 and Kt_4 was found to be from 32,000 to 39,000 KN·m/rad.

Table 1: Initial drive train information for torsional vibration analysis.

Class.	Component	Model	Sym	Value	
Moment of Inertia	G/Box Pinion	Disc 1	J_1	8.529	kgm^2
	Brake Disc	Disc 2	J_2	62.849	kgm^2
	Flange A	Disc 3	J_3	3.053	kgm^2
	Flange B	Disc 4	J_4	3.639	kgm^2
	Hub Disc	Disc 5	J_5	5.779	kgm^2
	Generator	Disc 6	J_6	120	kgm^2
Torsional Stiffness	Pinion shaft	Shaft 1	Kt_1	45,330	KN·m/rad
	Disc Pack 1	Shaft 2	Kt_2	-	KN·m/rad
	GFRP Tube	Shaft 3	Kt_3	-	KN·m/rad
	Disc Pack 2	Shaft 4	Kt_4	-	KN·m/rad
	Generator shaft	Shaft 5	Kt_5	54,800	KN·m/rad
Distance	Pinion shaft	Shaft 1	L_1	151	mm
	Disc Pack 1	Shaft 2	L_2	134	mm
	GFRP Tube	Shaft 3	L_3	1,199	mm
	Disc Pack 2	Shaft 4	L_4	177	mm
	Generator shaft	Shaft 5	L_5	125	mm
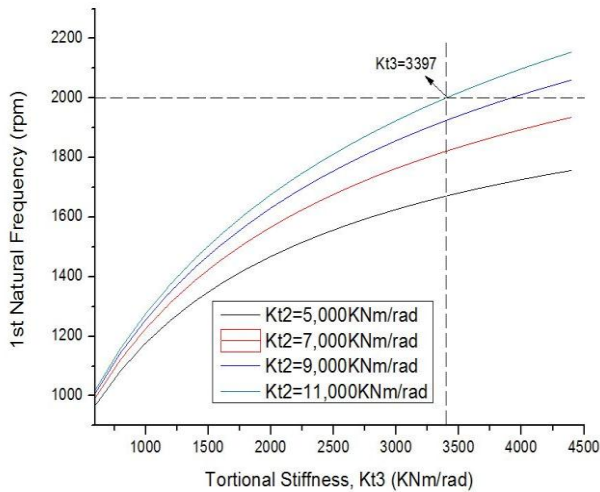
Figure 3: Critical speed map (Kt$_2$=5,000～11,000KN·m/rad)
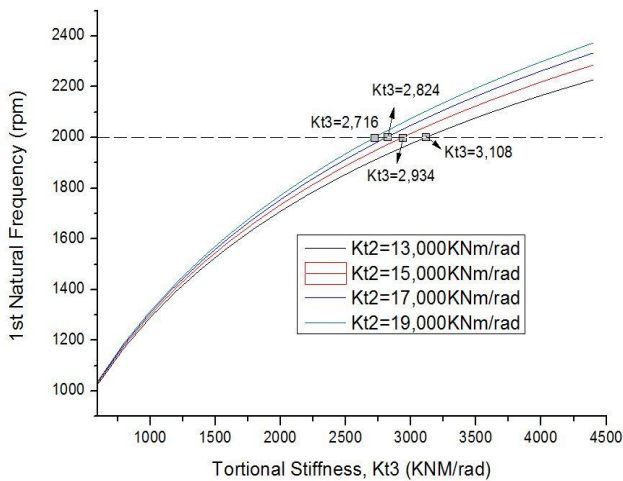
Figure 4: Critical speed map (Kt$_2$=13,000～19,000KN·m/rad)
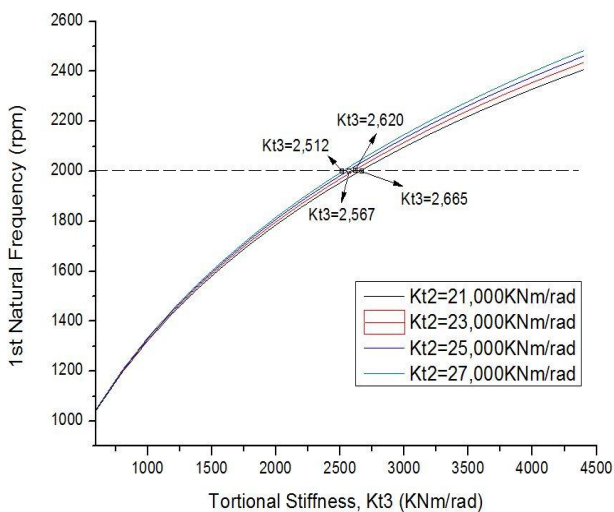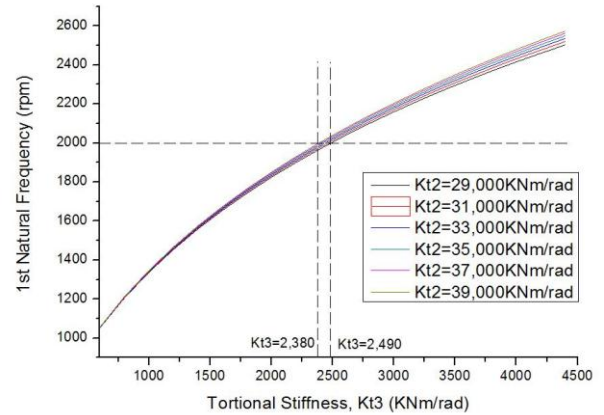

Figure 5: Critical speed map (Kt$_2$=21,000～27,000KN·m/rad)

Figure 6: Critical speed map (Kt$_2$=29,000～39,000KN·m/rad)

Calculation of Disc Pack and GFRP Tube Stiffness Values

To cause the GFRP spacer stiffness to be from 2,400 to 2,500 KN·m/rad, the variation of the stiffness depending on the GFRP tube thickness was calculated using finite element analysis [4]. The properties of the GFRP tube, including the stiffness and elastic modulus in different directions, were obtained by performing tensile testing at 0° and 90°. The experimental results were values of E1=43.3 GPa, E2=12.1 GPa, v_{12}=0.294, and G12 = 4.64 GPa. In addition, the tensile strength of a specimen laminated in conditions of [±55°] (236.7 MPa) was obtained by tensile testing.

The thickness of one ply produced by the filament winding method was assumed to be 0.5 mm; a design thickness of 10 mm was prepared at a lamination angle of [±55°]. Table 2 shows the orthotropic elasticity of the ply at a lamination angle of 0°.

**Table 2:** Orthogonal material properties of filament wound composite for finite element analysis

	Symbol	Unit	Values
Young's Modulus	E_x	GPa	12.0
	E_y	GPa	20.2
	E_z	GPa	12.1
Shear Modulus	G_{xy}	GPa	14.5
	G_{yz}	GPa	4.65
	Gzx	GPa	4.66
Poisson Ratio	v_{xy}	-	0.39
	v_{yz}	-	0.49
	v_{zx}	-	0.29

Finite element analysis was performed at tube thicknesses of 6 T to 10 T: a fixed boundary condition was applied to one side
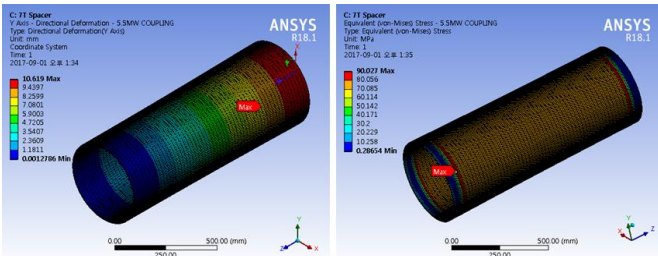
of the tube and a maximum torque of 86,000 Nm was applied to the other side of the tube. Finite element analysis was performed using the ANAYS 17.2 software. Figure 7 shows the equivalent stress and deformation under individual conditions.
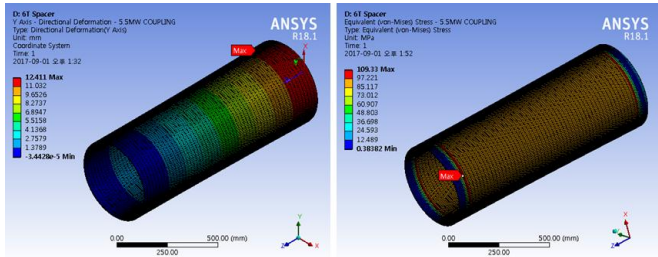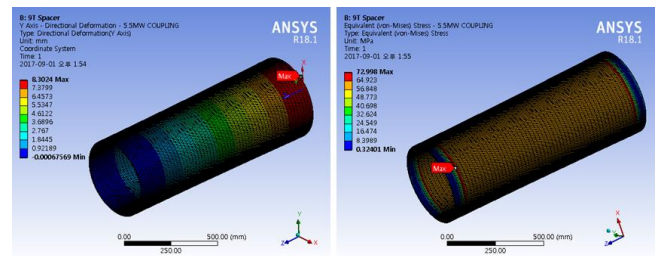

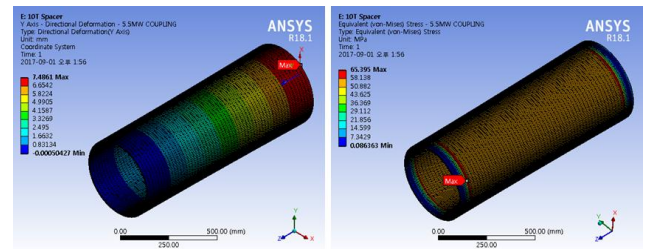(a) Deformation and Von-Mises Stress of GFRP Spacer (Thickness 6T)
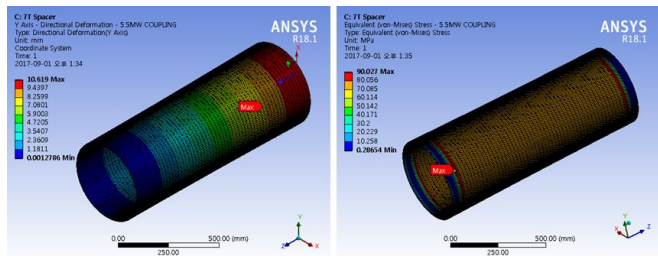
(b) Deformation and Von-Mises Stress of GFRP Spacer (Thickness 7T)

(c) Deformation and Von-Mises Stress of GFRP Spacer (Thickness 8T)

(c) Deformation and Von-Mises Stress of GFRP Spacer (Thickness 9T)

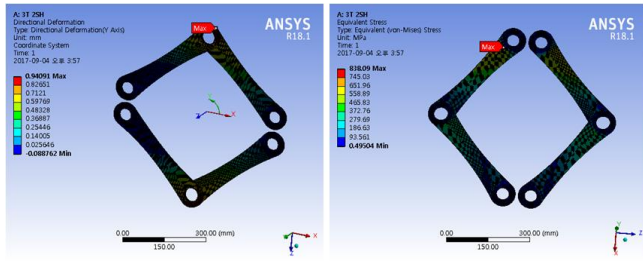(c) Deformation and Von-Mises Stress of GFRP Spacer (Thickness 10T)

Figure 7: Equivalent stress and deformation values for each analysis case (GFRP Spacer)

Table 3 summarizes the analytical results, which are the torsional stiffness values depending on the GFRP spacer thickness and the safety factors at a tensile strength of 211 MPa. When the thickness was 10 T, the torsional stiffness of the GFRP spacer was 2,491 KN·m/rad and the safety factor was 3.2. The optimal torsional stiffness of the GFRP spacer, obtained using the design described above, was from 2,400 to 2,500 KN·m/rad, which was verified to be an appropriate range.

Table 3: Stiffness and safety factor depending on the GFRP tube thickness.

| Case	6 T	7 T	8 T	9 T	10 T
Deformation [mm]	12.411	10.619	9.3041	8.3024	7.4861
Radius [mm]	214.75	215.25	215.75	216.25	216.75
Angle [rad]	0.057729	0.049293	0.043098	0.038374	0.034524
Maximum Torque [Nm]	86,000	86,000	86,000	86,000	86,000
Torsional Stiffness [KN·m/rad]	1,490	1,745	1,995	2,241	2,491
Equivalent Stress [MPa]	109.33	90.027	79.524	72.998	65.395
Safety factor	1.9	2.3	2.6	2.9	3.2

For the optimal design of the safety factor and the stiffness of the laminated disk pack of SPS6 material under the operating conditions, the equivalent stress and the stiffness of the disc pack were analyzed for cases in which the SPS6 material disc packs having thickness of 3T were laminated in two, three, and four layers. The mechanical properties of the SPS6 material used for the finite element analysis were evaluated using Young's modulus and Poisson's ratio. For the loading condition, a maximum torque of 86,000 Nm was applied, as in the case of the GFRP tube analysis. Figure 8 shows the equivalent stress and the deformation, calculated by finite element analysis.

(a) Deformation and Von-Mises Stress of Disc Pack

(Thickness 3T, 2Lamina)
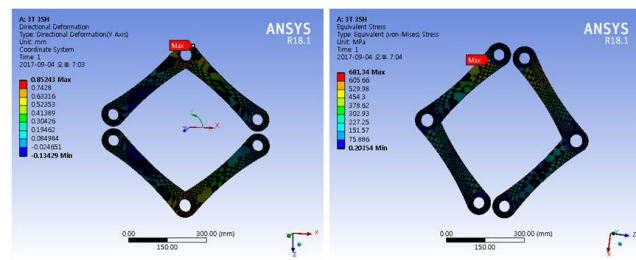
(b) Deformation and Von-Mises Stress of Disc Pack

(Thickness 3T, 3Lamina)
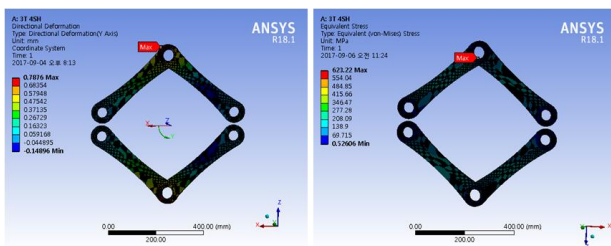
(c) Deformation and Von-Mises Stress of Disc Pack

(Thickness 3T, 4Lamina)

Figure 8: Equivalent stress and deformation amount for each analysis case (STS6 Disc Pack)

Table 4 shows the results of the finite element analysis and the safety factors at the yield strength of 1080 MPa. The safest case was when the thickness was 3 T and the number of the layers was three, as the safety factor was at its highest value of 1.6. In the case of 3T and three layers, the torsional stiffness was 33,798 KN·m/rad. Since range of the optimal disc pack torsional stiffness obtained using the design described above was from 32,000 to 39,000K KN·m/rad, the result was verified to be appropriate. Therefore, the appropriate choice is three layers of disk pack having a thickness of 3T.

**Table 4:** Torsional stiffness and safety factor depending on the disc pack thickness.

Case	3 T, 2 SH	3 T, 3 SH	3 T, 4 SH
Deformation [mm]	0.94091	0.85243	0.7876
Radius [mm]	335	335	335
Angle [rad]	0.002809	0.002545	0.002351
Maximum Torque [Nm]	86,000	86,000	86,000
Torsional Stiffness [KN·m/rad]	30,619	33,798	36,580
Equivalent Stress [MPa]	838.09	681.34	623.22
Safety factor	1.3	1.6	1.7

## Analysis of Eigenvalues of High-Speed Coupling

Using ANSYS software, the disk pack and GFRP tube stiffness model described above was used to analyze the eigenvalues of the high-speed coupling. Table 5 shows the information used for the eigenvalue analysis and the critical speed analysis. Figure 9 shows the eigenvalue analysis results obtained using ANSYS software in Modes 1 to 3. The natural frequency values obtained in the eigenvalue analysis were 36.68 Hz, 134.25 Hz, and 143.64 Hz in Modes 1 to 3, respectively.
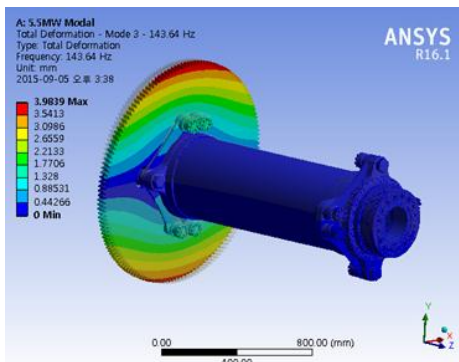
Table 5: Technical information

Description	Value
Maximum torque [Nm]	86,000
Maximum speed [rpm]	1,500
Operating speed [rpm]	350～1,300
Axial misalignment [mm]	± 10
Radial misalignment [mm]	≤25
Angular misalignment [°]	≤1.0
GFRP tube torsional stiffness [KN·m/rad]	2,491
Disc pack torsional stiffness [KN·m/rad]	33,798
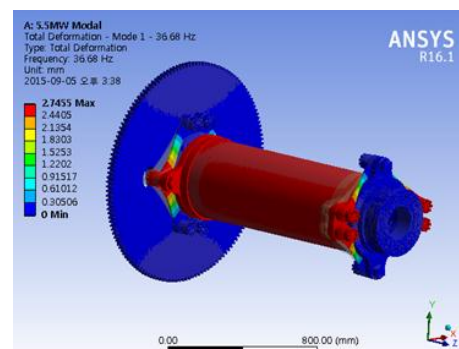
(a) First mode shape (36.68Hz)
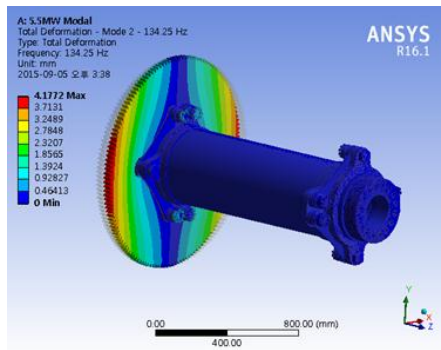
(b) Second mode shape (134.25Hz)

(c) Third mode shape (143.64Hz)

Figure 9: 1~3th Mode shape by modal analysis

Critical Speed Analysis

The operating speed of the high-speed coupling for wind power generators used in the present study was from 350 to 1300 rpm. Hence, critical speed analysis was performed by keeping the operating speed in the range of 350 to 1300 rpm. Figure 10 shows the results of the critical speed analysis with regard to excitation by mass imbalance. Figure 10 indicates the absence of a critical speed in the operating speed range. In addition, no critical speed was found below 2,000 rpm, indicating that the design was safe.
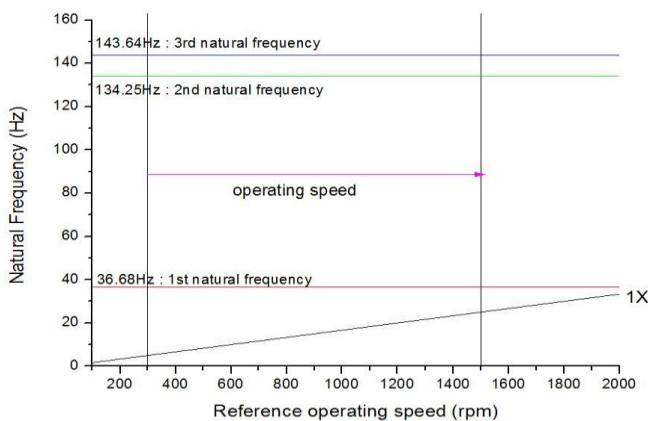

Figure 10: Campbell diagram

CONCLUSION

For the torsional stiffness parameter design of a GRFP spacer and a disc pack of a high-speed coupling for 6 MW wind power generators, vibration modeling of the high-speed coupling was performed using the transfer matrix method so as to cause the first natural frequency to be over 2,000 rpm.

1) Since the stiffness of the GRFP spacer was difficult to increase, the optimal torsional stiffness design was performed by keeping the disc pack stiffness high and the GRFP spacer stiffness low.

2) The following result was obtained from the high-coupling parameter design performed by varying the disc pack torsional stiffness from 5,000 to 39,000 KN·m/rad and the GFRP spacer torsional stiffness from 600 to 4,400 KN·m/rad. When the GFRP spacer torsional stiffness was from 2,400 to 2,500 KN·m/rad and the disc pack torsional stiffness was 32,000 to 39,000 KN·m/rad, the first natural frequency was over 2,000 rpm.

3) To keep the GFRP spacer stiffness in a range from 2,400 to 2,500 KN·m/rad in this design, the GFRP spacer torsional stiffness depending on the GFRP tube was analyzed. The results showed that at a thickness of 10 T the GFRP spacer stiffness was 2,491 KN·m/rad and the safety factor was 3.2. In addition, to keep the disc pack torsional stiffness in a range from 32,000 to 39,000 KN·m/rad in this design, the disc pack stiffness depending on the disc pack thickness was analyzed. The result showed that the disc pack torsional stiffness was 33,798 KN·m/rad when three disc packs having thickness of 3 T were laminated.

4) ANSYS modeling and critical speed analysis were performed with a product having GFRP spacer torsional stiffness of 2,491 KN·m/rad and disc pack torsional stiffness of 33,824 KN·m/rad; the result showed that no critical speed was found at the maximum operating speed of 1,500 rpm, and that the first natural frequency was over 2,000 rpm.

ACKNOWLEDGEMENT

REFERENCES

[1] "Wind turbines - Part 1: Design requirements", 2005, IEC61400-1 "Guideline for the Certification of Wind turbines", 2010, Germanischer Lloyd

[2] "Power transmission engineering, Flexible shaft couplings - Parameters and design principles", 1975, DIN740 Part 2.

[3] H.W Lee etc., 2016," A study on high speed coupling

design for wind turbine using a finite element analysis",
Journal of Mechanical Science and Technology, Vol.30,
No.8, pp.3713~3718

[4] J.H Kang etc., 2014, "Development of high speed
coupling for 2MW class wind turbine", Journal of the
Korean Society of Marine Engineering, Vol. 38, No. 3,
pp. 262~268

[5] "Flexible   Couplings   -Keyless   Fits",   1991,
ANSI/AGMA 9003-A91.

[6] B.J Hamrock and B.O Jacobson, 1999, "Fundamentals
of Machine Elements", 3rd Edition, McGraw-Hill

[7] Jon R. Mancuso, 1999, "Couplings and Joints-Design,
Selection   and   Application",   2nd   Edition,   Marcel
Dekker, Inc.

[8] J.S. Wu, 2013, "Analytical and Numerical Methods for
Vibrational Analyses", John Wiley and sons.

[9] Chao-Yang   Tsai   and   Shyh-Chin   Huang,   2013,
"Transfer matrix method to vibration analysis of rotors
with   coupler   offsets",   Shock   and   Vibration   20,
pp.97~108

[10] Qing He. and Dongmei Du, 2010, "Modeling and
Calculation   Analysis   of   Torsional   Vibration   for
Turbine Generator Shafts", Journal of Information &
Computational Science 7: 10 pp.2174~2182

[11] S.H. Ju, D.H. Kim etc, 2015, "Development and
Evaluation for the Insulated Coupling Test Machine of
a   Large   Wind   Turbine",   KWEA   proceedings,
pp.273~285. (in Korean)